# Opto-impedance characteristics of europium doped strontium aluminate and strontium chloro-apatite phosphors: a comparison

## K A Z Syed, P Kaleeswari, J Thirumalai, S P Manoharan, A Sundara Raj and R Jagannathan[1]

Central Electrochemical Research Institute, Karaikudi-630006, TN, India

E-mail: jags57_99@yahoo.com

## Abstract

Opto-impedance characteristics of the long persistent strontium aluminate : $Eu^{2+}$ phosphor system have been compared with fluorescent strontium chloro-apatite : $Eu^{2+}$ phosphor. This study has shown that optical pumping on the long persistent phosphor sample leads to a type of charge build-up and subsequent dispersion through a diffusion process occurring on a slow time scale ($\sim$s) centring on the $Dy^{3+}$ ion in agreement with a three-level scheme based on $Dy^{3+}$ related hole-trapping–detrapping mechanism.

(Some figures in this article are in colour only in the electronic version)

## 1. Introduction

Luminescent systems activated with europium (both divalent and trivalent ions) can cover the entire visible spectrum facilitating a wide gamut of applications ranging from luminescent lighting, CTV displays to luminescent immuno-assay labelling [1, 2]. Also digital radiographic storage phosphor systems for direct digital image acquisition have gained much attention in recent times [3]. Divalent europium doped strontium chloro-apatite [$Sr_5(PO_4)_3Cl$] and strontium aluminate [$SrAl_2O_4$] are two important photo-luminescent systems (respectively, labelled as SCAP and SAL in this paper) which upon excitation using UV radiation emit in the blue ($\lambda = 440$ nm) and bluish green regions ($\lambda = 510$ nm) exhibiting intense fluorescence and phosphorescence characteristics.

Their fluorescent and phosphorescent characteristics have been well explained using two- and three-level schemes in conjunction with the $f$–$d$ configuration coordinate model [4, 5]. Furthermore, optical pumping usually employed to activate fluorescence/phosphorescence processes in these samples may significantly modify the complexion of relaxation of the excited trap states that would eventually result in significant changes in photo-conductivity and allied photo-physical processes. We consider that investigations using the opto-impedance probe may add further insights related to the difference in relaxation mechanisms concerning the excited sub-band gap trap states related to $Eu^{2+}$ centres and might facilitate a better picture on the relaxation mechanisms (limited to the micro- or millisecond regime) involved. Hence, we believe that this study could supplement the current understanding on the subject hitherto not possible.

## 2. Experimental

Experimental procedures related to that of sample synthesis employing the solid state reaction method and the sample compositions were the same as given by our group earlier and by Matzuzawa *et al* [6, 7]. For details on optical and opto-impedance measurements we followed the same procedure as described earlier [8]. The concentration of divalent europium was kept at 2 mole% in both SCAP and SAL samples. In order to ascertain the role of $Dy^{3+}$ ions in

---

[1] Author to whom any correspondence should be addressed.
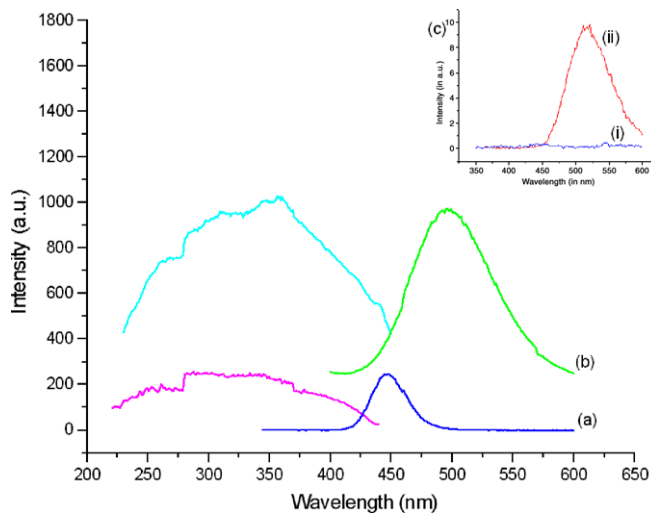
**Figure 1.** PL spectra for (*a*) strontium chloro-apatite doped with Eu$^{2+}$ (2 mole%) and (*b*) strontium aluminate doped with Eu$^{2+}$, Dy$^{3+}$ (SAL-1). The inset (*c*) shows the phosphorescence spectra for the same samples with decay time set at 2 s with (i) SCAP and (ii) SAL-1.

the phosphorescence related relaxation mechanism, many SAL samples with different concentrations of Dy$^{3+}$ in the range 0.05–0.10 mole with respect to the Sr-mole were prepared and investigated. However, in this paper for the sake of conciseness results corresponding to 0.05 mole and 0.10 mole Dy$^{3+}$ doped SAL samples, respectively, represented as SAL-1 and SAL-2 as examples are discussed.

## 3. Results

Upon UV excitation ($\lambda_{exc} \sim 360$ nm) divalent europium doped in these matrices (both strontium chloro-apatite and strontium aluminate) yields a narrow band photo-luminescence emission in the blue–bluish green region (440–510 nm). Figure 1 gives fluorescence and phosphorescence spectra of representative SCAP and SAL samples in each case. Although both SCAP and SAL samples yield intense photo-luminescence emission, the SCAP sample does not yield any phosphorescence emission at all (inset of figure 1).

Nyquist type opto-impedance plots for the SCAP and SAL-1 samples under investigation are given in figures 2 and 3. On comparison we see that under dark conditions both samples behave similarly with respect to exhibiting two semi-circular patterns in mid-(kHz) and high-(MHz) frequency regions. Interestingly the phosphorescent europium doped aluminate (SAL) system upon UV pumping shows different behaviours in that a pronounced linear feature appears in the low frequency (∼0.2 Hz) side (figure 3). More importantly, a totally distinct picture emerges in the case of sample SAL-2 having a higher Dy$^{3+}$ content. That in the impedance pattern semi-circular feature is completely lost; instead, we can observe the impedance points run nearly parallel to the *y*-axis representing the imaginary part of the complex impedance plot (figure 4).
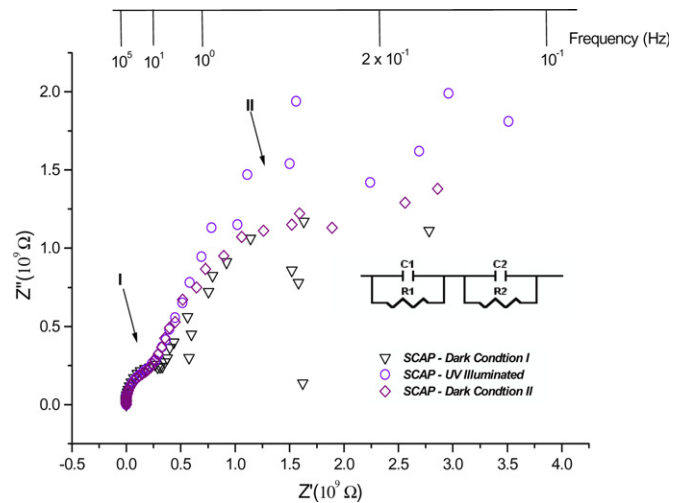


**Figure 2.** Nyquist impedance plots for SCAP under various illumination conditions. The inset shows the circuit model used for fitting impedance parameters. Frequency regions indicated for the Nyquist plot correspond to UV-illuminated SCAP.
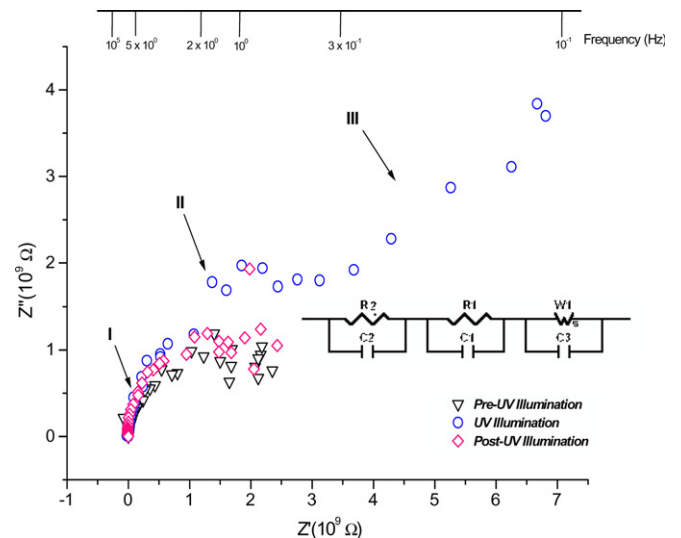


**Figure 3.** Nyquist impedance plots for SAL under various illumination conditions. The inset shows the circuit model used for fitting impedance parameters for UV-illuminated SAL. Frequency regions are marked for the Nyquist plot for UV-illuminated SAL.

## 4. Discussion

In a luminescent matrix doped with divalent europium, the band emission can be assigned to an *f*–*d* allowed electric dipole transition [9, 10]. An allowed electric dipole transition due to Eu$^{2+}$ ions in these matrices might yield a fluorescent lifetime in the microsecond regime [11]. This corresponds to the MHz region in the frequency scale if any direct signature of these processes would be possible. It should be noted that upon UV excitation, in the case of the strontium chloro-apatite : Eu$^{2+}$ system we can observe only photo-luminescence emission, whilst the strontium aluminate : Eu$^{2+}$ counterpart exhibits intense phosphorescence features spanning to a few seconds as depicted in the inset of figure 1. Considering various photo-physical processes
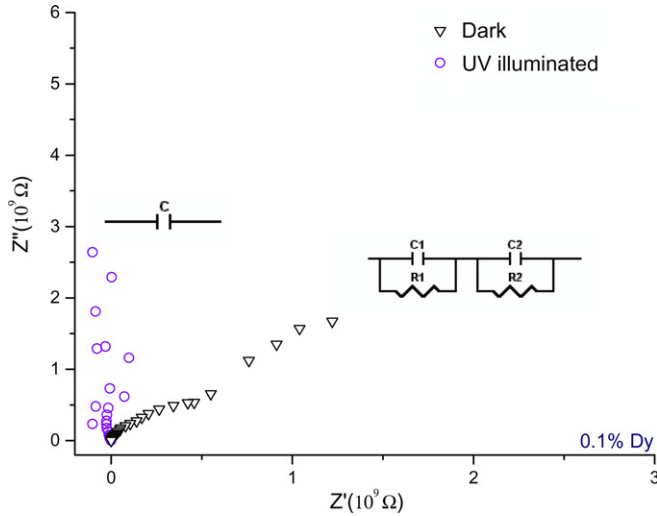
**Figure 4.** Complex plane impedance plots for the SAL-2 system with a higher dysprosium content. Equivalent circuits used to fit are shown near the corresponding impedance plots.

following optical pumping on the systems in turn, we have that in the case of strontium chloro-apatite : $Eu^{2+}$ exhibiting just photo-luminescence characteristics, a two-level scheme would suffice to describe the non-persistent fluorescence processes. On the other hand, for the phosphorescent strontium aluminate : $Eu^{2+}$ system we need to invoke the three-level scheme wherein the presence of sub-band gap traps should be taken into consideration [12]. Turning to explain the results of opto-impedance study, from conventional impedance spectroscopy [13] we have that a parallel resistor–capacitor combination will result in a semi-circular impedance pattern under a Nyquist type plot.

In order to explain the two semi-circles observed we may consider different possibilities as follows:

(i) silver contacts used to establish electrical contacts with the ceramic material as the dielectric held in between resembles the geometry of a parallel plate capacitor in conjunction with the bulk resistance of the material constituting a parallel RC combination,

(ii) the drift and diffusion of the defect complexes generated due to oxygen off-stoichiometry arising out of heat-treatment conditions in solid state synthesis, and

(iii) the drift and diffusion of the defects generated due to $Sr^{2+}$ vacancies or $Dy^{3+}$ related hole traps.

Nevertheless, the observation of two semi-circles in the Nyquist impedance plot suggests the presence of two independent resistor–capacitor parallel networks (indicated as $R1$, $C1$, $R_2$ and $C_2$). We consider that this may arise from either of the first two possibilities listed above. In the same fashion for both fluorescent and phosphorescent samples we can ascribe the two semi-circles observed to silver contacts with the dielectric fluorescent/phosphorescent materials sandwiched across making a parallel resistor–capacitor combination. These two kinds of ceramics will have different electronic conductivities and hence their bulk resistivities may differ considerably having a modest influence

on photo-shining on these samples resulting in a semi-circular pattern (region marked I). Secondly, the defect centres generated on account of oxygen off-stoichiometry could generate some sort of photo-physical processes resulting in a significant modification of the opto-impedance pattern (region marked II). A most important result concerning the opto-impedance study on these materials is the emergence of a third region having a linear profile occurring in the low frequency region (~mHz) indicating a relatively slow process occurring through a diffusion type process. It may be of relevance to note here that a simple $(R_1C_1)(R_2C_2)$ equivalent circuit model (given in the inset of figure 2) suffices to fit the impedance parameter values obtained for SCAP, whereas a more complicated $(R_1C_1)(R_2C_2)(W_1C_3)$ model (inset of figure 3) is required to fit the impedance values for the optically excited SAL system substantiating the presence of complex photo-physical processes occurring within the bulk.

In order to arrive at a semi-quantitative picture of the photo-physical processes that follows the optical pumping we have that

(i) in the case of fluorescent SCAP it seems to be straightforward. Because from table 1 giving the various fitted parameters both under dark and UV shined conditions, we could not see any spectacular change in the opto-impedance parameters, except for a modest change (~10%),

(ii) whilst in the case of the SAL system the changes are spectacular (⩾50%) and are more complex indicating the multiplicity of intense photo-physical processes.

For the sake of conciseness, we restrain from discussing the results of SCAP except using them for comparison. Furthermore even in the case of the SAL system for all practical reasons we can ignore region I, which does not seem to indicate any significant light dependent photo-physical processes.

Recently Jia [12] had described about various photo-physical processes involved during the course of optical pumping on this lone phosphorescent system on the basis of a three-level system. The relaxation via the trap state can be described by

$$\frac{dN_{trap}}{dt} = C_{trap}N_{exctd} - C_{detrap}N_{trap} \tag{1}$$

with $N_{exctd}$ and $N_{trap}$ the number of $Eu^{2+}$ excited and trap states and $C_{trap}$ and $C_{detrap}$ the trapping and de-trapping rates, respectively. In this system relaxation of energy via trap states lying in the sub-band gap region is more complex owing to the multiplicity of the trap states.

The trap state lying in the mid-gap region of the SAL system can have different origins due to shallow and deep traps due to Sr-vacancy, hole traps related to $Dy^{3+}$ centre(s) with traps located at 0.19, 0.41 and 0.57 eV [12]. Notwithstanding the multiplicity of traps in the SAL system, the relaxation of excited energy through after-glow phosphorescence emission has been established to be mono-molecular and in the time regime of few seconds. Simultaneously it should be borne in mind that direct relaxation from the europium excited state

**Table 1.** Fitted impedance parameters for SCAP and SAL-1 systems.

| System | Condition | Region I | | | Region II | | | Region III | | | |
| | | | | | | | | $W_1$ | | | |
| | | $R_1$ (MΩ) | $C_1$ (pf) | $\tau_1$ (ms) | $R_2$ (MΩ) | $C_2$ (pf) | $\tau_2$ (ms) | W-R (MΩ) | W-T (s) | W-P | $C_3$ (pf) |
| Strontium aluminate : Eu$^{2+}$ SAL - 1 | Dark I | 1739 | 49 | 85 | 1330 | 954 | 127 | — | — | — | — |
| | 254 nm Optical pumping | 3054 | 109 | 330 | 1450 | 48 | 70 | 5260 | 2.2 | 0.58 | 500 |
| | Dark II | 1387 | 47 | 66 | 1760 | 315 | 554 | — | — | — | — |
| Strontium chloro-apatite : Eu$^{2+}$ | Dark I | 443 | 30 | 13 | 2060 | 265 | 547 | — | — | — | — |
| | 254 nm Optical pumping | 406 | 37 | 15 | 3662 | 169 | 620 | — | — | — | — |
| | Dark II | 474 | 52 | 25 | 2637 | 251 | 661 | — | — | — | — |

*Note:* Dark I—initial dark condition; dark II—dark condition after UV shining measurements.

working with an allowed electric dipole transition mechanism would be in the microsecond regime [11].

It turns out that the case of fluorescent SCAP is simple in that there is no spectacular change in the opto-impedance spectra both in terms of pattern and magnitude, while the phosphorescent SAL system shows a significant change. That is, in addition to the two semi-circular parts undergoing significant modification under UV pumping there is the emergence of an additional linear component in the low frequency end (∼0.4–0.2 Hz) as already pointed out. Accordingly one may ascribe a simple *RC* parallel combination to each semicircle and a Warburg circuit element to the linear part. The significant change (enhancement) in *R* and *C* values observed for both regions (I and II) might suggest the continuance of the same processes even under optical pumping as under dark conditions but with modified parameters. We can see from table 1 that for the SAL system for region I both resistance and capacitance ($R_1$, $C_1$) values increase, while for region II there is a considerable decrease only in the capacitance ($C_2$) value. Canonically we can rationalize the increase in resistance in terms of different defects generated leading to increased ohmic resistance and modification of the charge gradient influencing the capacitance values; the pronounced (one order) decrease observed in the capacitance value under region II is rather surprising. Another important point that should be noted here is that the time constants of these impedance profiles are centred at the low frequency region (∼10 Hz). Hence, obviously these features cannot be attributed to the relaxation of the Eu$^{2+}$ excited state working with an allowed electric dipole transition mechanism which usually occur in the microsecond regime. Hence, for all practical purposes, we can ignore contributions from any direct transitions between the ground and excited states. Alternatively these features involving essentially slow kinetics can be fixed to trap states in the sub-band gap region in the vicinity of Dy$^{3+}$ centre(s). It should be borne in mind that electronic transitions centring on Dy$^{3+}$ involving parity forbidden $f$–$f$ transitions would be in the millisecond time scale. Hence, it seems reasonable to expect that transitions

originating from or occurring via the intermediate trap state are more important in explaining the present results.

Electronic transitions centring on the trap states will mostly be hole traps related to Dy$^{3+}$ centres, notwithstanding there will be some vacancy-related defects. Although various defects are distributed in the sub-band gap region with an energy spacing of ∼0.3 eV, this follows a mono-molecular relaxation mechanism [12].

It is known that in this phosphorescent (SAL) system both europium (Eu) and dysprosium (Dy) species involve a charge transfer (valence change) complex with oxygen species. This may lead to some sort of charge build-up eventually resulting in a configuration resembling two separate resistor-parallel combinations thus accounting for the presence of two semi-circles (regions I and II). Reasons being manifold, namely, there is a profound photo-induced enhancement in the charge build-up as indicated by the increase in capacitance, the two semi-circles (regions I, II) occur in a relatively faster time scale than region III but yet in the millisecond regime (to be consistent with $f$-type ions). On the other hand, the linear region in the low frequency end (region III) occurs more slowly (in a time span of a few seconds). In stark contrast to region I, there is a marked photo-induced decrease in the capacitance for region II, hence suggesting an obvious decrease in the electrical charge.

Results of samples with a higher concentration of Dy$^{3+}$ (two times more than the optimized concentration) corroborate our hypothesis that in the vicinity of Dy$^{3+}$ centres, there may be some kind of charge-build up. From figure 4 and table 2, we can infer that for SAL-2 having a higher Dy concentration there is virtual freeze of the flow of charges consequent to UV shining. We can observe a spectacular one-dimensional shooting of impedance values parallel to the *y*-axis which is a clear indication of the increase in the capacitive impedance which works out to be about three fold. Furthermore, a colossal increase in the resistive impedance observed (table 2) is again in support of our hypothesis that charges are localized, a situation that would mimic the freezing of charges entailing in the absence of charge flow to rationalize the colossal increase in the resistance observed under UV shined conditions. Also it is

**Table 2.** Fitted impedance parameters for SAL-1 and SAL-2 systems.

| | | Impedance parameters ( fitted ) | | | | | | | | | | |
| | | Region I | | | Region II | | | Region III | | | | |
| | | | | | | | | $W_1$ | | | | |
| System | Condition | $R_1$ (MΩ) | $C_1$ (pf) | $\tau_1$ (ms) | $R_2$ (MΩ) | $C_2$ (pf) | $\tau_2$ (ms) | W-R (MΩ) | W-T (s) | W-P | $C_3$ (pf) | Remarks |
| Strontium aluminate : $Eu^{2+}$ SAL-1 | Dark I | 1739 | 49 | 85 | 1330 | 954 | 127 | — | — | — | — | |
| | 254 nm Optical pumping | 3054 | 109 | 330 | 1450 | 48 | 70 | 5260 | 2.2 | 0.58 | 500 | [a] |
| | Dark II | 1387 | 47 | 66 | 1760 | 315 | 554 | — | — | — | — | |
| Strontium aluminate : $Eu^{2+}$ SAL-2 | Dark I | 463 | 48.67 | 23 | 7420 | 133 | 987 | — | — | — | — | |
| | 254 nm Optical pumping | $6.955 \times 10^{16}$ | 12832 | $9 \times 10^{17}$ | — | — | — | — | — | — | — | [b] |

[a] Large increase in capacitance in the low frequency region.

[b] The response becomes entirely capacitive.

important to note that this whole process occurs more slowly than does the case of sample SAL-1 doped with a nominal amount of $Dy^{3+}$ as indicated by the several orders of increase in the time constant ($\tau_1$) in sample SAL-2. This clearly fixes the origin of the temporal charge build-up under UV shined conditions to Dy-related centres.

Furthermore, in impedance spectroscopy, a line-type impedance profile would indicate a Warburg-type diffusion process, essentially involving the flow of charge [13]. It is reasonable that the flow of charges essentially means the decrease in the charge build-up thus explaining the pronounced photo-induced decrease in the capacitance for region III. It is pertinent to note here that the motion of thermally activated holes in the valence band (figure 5) via a trapping –de-trapping mechanism centred on Dy-related traps is a process occurring in a low time scale [14]. The presence of defects might generate a diffused band edge localized in the vicinity of Dy centres which may be a thermally activated diffusion process.

Hence we can say that the opto-impedance results of the present investigation are consistent with the three-level scheme proposed for explaining phosphorescence in the celebrated SAL system [12]. So the substantial variation in the fitted impedance parameter values on UV illumination and post-illumination conditions for the SAL system may be attributed to the complexity of trapping–detrapping kinetics dictated by the presence of multiple traps in the sub-band gap region. This may be compared with the photo-charging parameters reported by Jia [12], where a wide variation (about an order of magnitude) is observed among the strength and frequency parameters under low-illumination and high-illumination conditions.

Fitted parameters corresponding to region III representing the Warburg part for the UV excited SAL system (table 1) reflect that the diffusion process takes place in the time scale of ~2.2 s. We assume the diffusion coefficient ($D$) value of $6 \times 10^{-12}$ m$^2$ s$^{-1}$ [15] corresponding to hole related traps arising from the oxygen defect with the Kroger–Vink label $V_O$
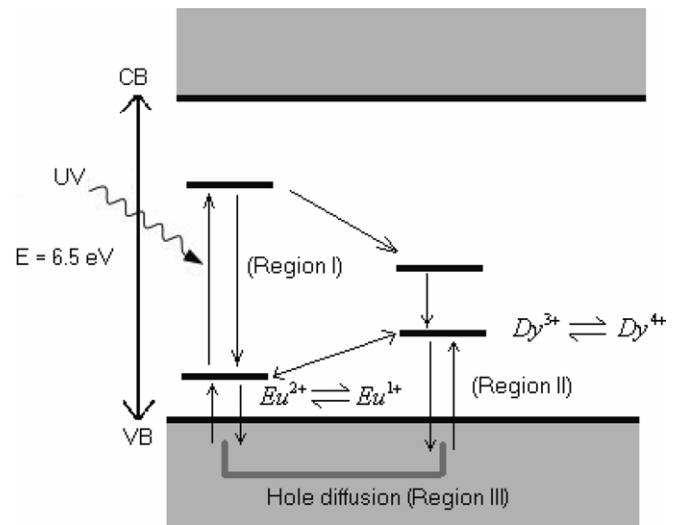


**Figure 5.** Schematic illustrating various photo-physical processes in the SAL system upon optical pumping.

in the alumina matrix in close comparison with the SAL system under study. Using this value in the well-known relation $L \sim (Dt)^{1/2}$, we find that the diffusion length ($L$) for the hole-trap complex through the background matrix of SAL is found to be ~3.5 $\mu$m. Although this value appears to be very high, we consider that a further detailed investigation is necessary which is in progress.

## 5. Conclusion

A comparison of opto-impedance data of fluorescent SCAP and long persistent SAL samples has shown that it is possible to pick up the photo-relaxation mechanism of the latter occurring in the millisecond–second time regime and the results are consistent with the three-level scheme based on $Dy^{3+}$ related hole-trapping–detrapping mechanism. This study has further

J. Phys. D: Appl. Phys. **41** (2008) 175412

K A Z Syed *et al*

indicated that the charge build-up and subsequent dispersion through a diffusion process occur in a slow time scale centring around the $Dy^{3+}$ ion.

## Acknowledgments

## References

[1] Blasse G and Grabmaier B C 1994 *Luminescent Materials* (New York: Springer)
[2] Degan P, Abbondandalo A and Montagnoli G 2005 *J. Biolumin. Chem. Lumin.* **5** 207
[3] Spaeth J M 2001 *Rad. Meas.* **33** 527
[4] Nakazawa E and Mochida T 1997 *J. Lumin* **72–74** 236
[5] Blasse G 1988 *Prog. Solid. State Chem.* **18** 79
[6] Jagannathan R, Rao R P, Narayanan R L and Srinivasan L K 1990 *Solid State Commun.* **74** 825
[7] Matsuzawa, Aoki Y, Takeuchi N and Murayama Y 1996 *J. Electrochem. Soc.* **143** 2670
[8] Kalyani P, Sivasubramanian S, Ragavendran K, Kalaiselvi N, Ranganathan N G, Madhu S, Sundararaj A, Manoharan S P and Jagannathan R 2005 *J. Phys. D: Appl. Phys.* **38** 990
[9] Blasse G 1973 *Phys. Status Solidi* b **55** K131
[10] Ryan F M, Lehmann W, Feldman D W and Murphy J 1974 *J. Electrochem. Soc.* **121** 1475
[11] Clabaua F, Rocquefeltea X, Jobica S, Deniarda P, Whangbob M, Garciac A and Le Mercierd T 2007 *Solid. State Sci.* **9** 608
[12] Jia D 2003 *Opt. Mater.* **22** 65
[13] Barsoukov E, Macdonald R (ed) 2005 *Impedance Spectroscopy: Theory, Experiment and Applications* (New York: Wiley)
[14] Jia W, Yuan H, Lu L, Liu H and Yen W M 1998 *J. Lumin.* **76–77** 424
[15] Gray D E (ed) 1972 *American Institute of Physics Handbook* 3rd edn (New York: McGraw-Hill)